

**U-Load  
Dextramer®**

Build multimers with your choice of peptide and peptide-receptive MHC I and MHC II alleles.



This information is current as of February 26, 2022.

## Engagement of the Aryl Hydrocarbon Receptor in *Mycobacterium tuberculosis*–Infected Macrophages Has Pleiotropic Effects on Innate Immune Signaling

Babak Memari, Manuella Bouttier, Vassil Dimitrov, Marc Ouellette, Marcel A. Behr, Jorg H. Fritz and John H. White

*J Immunol* 2015; 195:4479-4491; Prepublished online 28 September 2015;  
doi: 10.4049/jimmunol.1501141  
<http://www.jimmunol.org/content/195/9/4479>

**Supplementary Material** <http://www.jimmunol.org/content/suppl/2015/09/28/jimmunol.1501141.DCSupplemental>

**References** This article **cites 68 articles**, 17 of which you can access for free at:  
<http://www.jimmunol.org/content/195/9/4479.full#ref-list-1>

**Why *The JI*? Submit online.**

- **Rapid Reviews! 30 days\*** from submission to initial decision
- **No Triage!** Every submission reviewed by practicing scientists
- **Fast Publication!** 4 weeks from acceptance to publication

*\*average*

**Subscription** Information about subscribing to *The Journal of Immunology* is online at:  
<http://jimmunol.org/subscription>

**Permissions** Submit copyright permission requests at:  
<http://www.aai.org/About/Publications/JI/copyright.html>

**Email Alerts** Receive free email-alerts when new articles cite this article. Sign up at:  
<http://jimmunol.org/alerts>



# Engagement of the Aryl Hydrocarbon Receptor in *Mycobacterium tuberculosis*-Infected Macrophages Has Pleiotropic Effects on Innate Immune Signaling

Babak Memari,\* Manuella Bouttier,\* Vassil Dimitrov,\* Marc Ouellette,\*  
Marcel A. Behr,<sup>†,‡,§,¶</sup> Jorg H. Fritz,<sup>\*,||,#</sup> and John H. White<sup>\*,†,§</sup>

Understanding the mechanisms of host macrophage responses to *Mycobacterium tuberculosis* is essential for uncovering potential avenues of intervention to boost host resistance to infection. Macrophage transcriptome profiling revealed that *M. tuberculosis* infection strongly induced the expression of several enzymes controlling tryptophan catabolism. These included IDO1 and tryptophan 2,3-dioxygenase, which catalyze the rate-limiting step in the kynurenine pathway, producing ligands for the aryl hydrocarbon receptor (AHR). The AHR and heterodimeric partners AHR nuclear translocator and RELB are robustly expressed, and AHR and RELB levels increased further during infection. Infection enhanced AHR/AHR nuclear translocator and AHR/RELB DNA binding and stimulated the expression of AHR target genes, including that encoding the inflammatory cytokine IL-1 $\beta$ . AHR target gene expression was further enhanced by exogenous kynurenine, and exogenous tryptophan, kynurenine, or synthetic agonist indirubin reduced mycobacterial viability. Comparative expression profiling revealed that AHR ablation diminished the expression of numerous genes implicated in innate immune responses, including several cytokines. Notably, AHR depletion reduced the expression of *IL23A* and *IL12B* transcripts, which encode subunits of IL-23, a macrophage cytokine that stimulates production of IL-22 by innate lymphoid cells. AHR directly induced *IL23A* transcription in human and mouse macrophages through near-upstream enhancer regions. Taken together, these findings show that AHR signaling is strongly engaged in *M. tuberculosis*-infected macrophages and has widespread effects on innate immune responses. Moreover, they reveal a cascade of AHR-driven innate immune signaling, because IL-1 $\beta$  and IL-23 stimulate T cell subsets producing IL-22, another direct target of AHR transactivation. *The Journal of Immunology*, 2015, 195: 4479–4491.

The innate arm of the immune system detects environmental pathogens and mounts a primary immune response. The aryl hydrocarbon receptor (AHR), which is activated by a range of ligands of environmental or dietary origin, has emerged

recently as an important regulator of innate immunity (1–3). It is a ligand-regulated transcription factor and member of the basic helix-loop-helix–PAS transcription factor family, whose homologs include its heterodimeric partner, the AHR nuclear translocator (ARNT). AHR/ARNT heterodimers recognize cognate DNA sequences known variously as xenobiotic, dioxin, or AHR response elements (AHREs) in target genes. Apart from the classic AHR/ARNT pathway, AHR controls gene expression via interaction with other transcriptional regulators, including RELB, an anti-inflammatory and immune-modulatory subunit of the transcription factor complex NF $\kappa$ B/AHR (4).

AHR was initially characterized for its capacity to bind dioxin (2,3,7,8-tetrachlorodibenzodioxin), a highly potent environmental toxin. Importantly, however, it also recognizes a wide variety of natural compounds of environmental origin with varying affinities, all of which are characterized by their planar structures. These include several normal dietary constituents or their metabolites (e.g., flavonoids and indoles in fruits and vegetables [quercetin in apples, resveratrol in grapes and red wine, indole-3-carbinols in cruciferous vegetables]) and components of teas, along with metabolites of the essential amino acid tryptophan (Trp) (3, 4). In addition, Trp catabolism down the kynurenine pathway produces AHR ligands and is initiated by tryptophan-2,3-dioxygenase (TDO2) and distinct, but biochemically related, IDO1 and IDO2 (5).

It appears paradoxical, at first glance, that components of a healthy diet and endogenously produced ligands activate the same signaling pathways as environmental toxins, such as dioxin. However, the immunotoxicity of dioxin arises from a combination of its high affinity for AHR and its accumulation and persistence

\*Department of Physiology, McGill University, Montreal, Quebec H3G 1Y6, Canada; <sup>†</sup>Department of Medicine, McGill University, Montreal, Quebec H3G 1Y6, Canada; <sup>‡</sup>Montreal General Hospital, McGill University, Montreal, Quebec H3G 1A4, Canada; <sup>§</sup>McGill International TB Centre, McGill University, Montreal, Quebec H3G 1A4, Canada; <sup>¶</sup>Division of Infectious Diseases and Medical Microbiology, McGill University, Montreal, Quebec H3G 1A4, Canada; <sup>||</sup>Department of Microbiology and Immunology, McGill University, Montreal, Quebec H3G 0B1, Canada; and <sup>#</sup>Complex Traits Group, McGill University, Montreal, Quebec H3G 0B1, Canada

ORCID: 0000-0002-4754-6217 (B.M.).

Received for publication May 19, 2015. Accepted for publication September 2, 2015.

This work was supported by operating grants from Genome Quebec and the Canadian Institute of Health Research to J.H.W. M.B. was supported by a fellowship from the Fonds de Recherche du Québec-Santé.

The sequences presented in this article have been submitted to Array Express under accession number E-MTAB-3192. The results of microarray analysis have been submitted to the National Center for Biotechnology Information Gene Expression Omnibus under accession number GSE70200.

Address correspondence and reprint requests to Dr. John H. White, McGill University, McIntyre Building, Room 1112, 365 Drummond Street, Montreal, QC H3G 1Y6, Canada. E-mail address: john.white@mcgill.ca

The online version of this article contains supplemental material.

Abbreviations used in this article: AHR, aryl hydrocarbon receptor; AHRE, AHR response element; ARNT, AHR nuclear translocator; ChIP, chromatin immunoprecipitation; ChIP-seq, ChIP-sequencing; HAA, 3-hydroxyanthranilic acid; H3K27Ac, H3K27 acetylation; H3K4me1, H3K4 monomethylation; ILC, innate lymphoid cell; IP, immunoprecipitation; qPCR, quantitative PCR; RT, reverse transcription; siRNA, small interfering RNA; TB, tuberculosis; TDO2, tryptophan-2,3-dioxygenase; Trp, tryptophan.

Copyright © 2015 by The American Association of Immunologists, Inc. 0022-1767/15/\$25.00

in the human body (3, 6, 7), as a result of its notorious resistance to metabolism; dioxin/AHR signaling leads to elevated hepatic conversion of procarcinogens into carcinogens, accelerating tumorigenesis. Importantly, endogenous AHR ligands derived from Trp do not exhibit the same toxicological profile as dioxin in vitro and in vivo (8), and blockage of the Trp-kynurenine pathway in mice leads to chronic granulomatous diseases whose symptoms can be alleviated by exogenous kynurenine (9). Trp metabolism to kynurenines was originally identified for its role in innate immune defense against infection. Both TLR and IFN- $\gamma$  signaling stimulate IDO1 expression (10), and the resulting kynurenine production can contribute to control of infection by intracellular parasites, such as *Toxoplasma gondii* and *Chlamydia trachomatis* (10).

Exposure to environmental AHR ligands occurs mostly via barrier organs (gut, lung, and skin), which are highly active immune sites. There is compelling evidence for a role for AHR in controlling innate immunity. It is expressed at high levels in NK cells (11) and subsets of innate lymphoid cells (ILCs) (12, 13), which are present in large numbers in epithelial surfaces that defend against environmental assaults. Expression of AHR is required for ILCs and NK cells to produce IL-22, which is an innate immune cytokine that stimulates epithelial cell production of antibacterial proteins and replenishes the mucosal layer, thus enhancing epithelial barrier function (14). Notably, *Ahr*-null mice display enhanced susceptibility to infection and to inflammatory bowel diseases (2, 15, 16).

Recent work showed that total or myeloid-specific depletion of AHR in mice enhances their sensitivity to *M. tuberculosis* infection, revealing a role for myeloid-specific AHR signaling in antimycobacterial defenses (17). We have been interested in characterizing in detail the primary host macrophage transcriptional responses to *M. tuberculosis* infection. *M. tuberculosis* has infected approximately two billion people worldwide (18), and tuberculosis (TB) kills approximately three people every minute (19). Although most are latently infected, active TB represents the leading cause of death from a curable disease (20). Although current treatments aim to control active disease or prevent progression of infection to disease, an attractive point of intervention would be at the transition from exposure to infection by enhancing innate control at the time of exposure. Innate immunity to *M. tuberculosis* is critical for determining disease outcome, and it has long been recognized that during TB outbreak investigations, only 30–50% of those with an equivalent exposure develop a productive infection, as demonstrated by a tuberculin skin-test conversion (21). Alveolar and recruited inflammatory macrophages are important myeloid cells in the lung and are infected by *M. tuberculosis*. Our transcriptome profiling studies in infected macrophages revealed that expression levels of *IDO1* and *TDO2* increase dramatically throughout the course of infection. This leads to engagement of AHR, and we find that AHR signaling has widespread effects on the innate immune responses mounted in infected cells against *M. tuberculosis*. Notably, AHR contributes to the expression of several cytokines and chemokines. These include IL-23, a macrophage cytokine required for long-term control of *M. tuberculosis* infection (22–24) that induces IL-22 production in barrier organs; this reveals that AHR signaling controls transcription of several components of the IL-23/IL-22 innate immune pathway.

## Materials and Methods

### THP-1 and *M. tuberculosis* cell culture

THP-1 cells (TIB-202; American Type Culture Collection) were cultured in RPMI 1640 (Wisent 350-005-CL) with 10% FBS (nonheat inactivated). H37Ra and H37Rv were maintained in log phase (OD<sub>600</sub> between 0.2 and 0.6) and cultured in a rolling incubator at 37°C in Middlebrook 7H9 Broth

(Difco) with 0.05% Tween-80 and 10% albumin, dextrose, catalase (BD Biosciences). To test for clumping, mycobacteria were grown to an OD<sub>600</sub> of 0.6 (concentration =  $0.6 \times 10^8$  bacteria/ml). One milliliter of bacterial culture was centrifuged for 5 min, 4000 rpm at room temperature, and the bacteria were resuspended in 2 ml RPMI 1640 and syringed 10 times through a 25G needle. A drop of 50  $\mu$ l was taken, and a smear of bacteria was done and stained with Prolong Gold (Life Technologies) containing DAPI. The bacteria were imaged with a fluorescence bright-field microscope (Axiovert; Zeiss) at 100 $\times$  magnification.

### Bone marrow-derived macrophages

Bone marrow macrophages were isolated from C57BL/6 mice femurs. On day 0, leg bones were clipped and cleaned, and two bone heads were opened with scissors. Bone was placed inside a 200- $\mu$ l PCR tube that had a needle-sized hole at the bottom. This tube was placed in a 1.5-ml vial containing 300  $\mu$ l sterile PBS. The hinges of 200- $\mu$ l vials were placed between the caps of 1.5-ml vials to hold them in place. Tubes were quickly spun, and the 200- $\mu$ l PCR tubes were removed. Bone marrow was resuspended and combined into two tubes and centrifuged at 2000 rpm for 5 min. Supernatant was removed, and 1 ml DMEM high-glucose medium containing 30% supernatant from cultured L929 mouse fibroblasts (a source of M-CSF) was added, and pellets were resuspended. The mixture was added to the total solution and plated in 10-ml aliquots. On day 2, 2 ml DMEM high glucose was added to each plate (from prepared solution, no L929-conditioned media). On day 3, 3 ml conditioned medium from L929 cells was added to each plate. On day 6, supernatant was removed from each plate and washed with 10 ml DMEM high glucose. A total of 10 ml fresh DMEM high glucose was added, cells were scraped into 10 ml DMEM high glucose and transferred to a 50-ml conical tube, and aliquots were obtained for cell counting.

### Human primary macrophage isolation and culture

Following informed written consent, blood was drawn from a healthy adult female donor. PBMCs were isolated, as previously described (25). Briefly, after PBMC isolation, monocytes were left to adhere to tissue culture dishes in RPMI 1640–10% FBS. Media were changed after 24 h, and monocytes were treated with GM-CSF (100 ng/ml) for 6 d, with media changes every 2 d. Protocols for the collection of blood for research purposes were approved by the Research Ethics Board of the McGill University Health Centre Research Institute.

### Macrophage infections

THP-1 cells were differentiated by PMA (Sigma), final concentration 100 ng/ml, for 24 h in RPMI 1640 supplemented with nonheat-inactivated 10% FBS. H37Ra cultures were centrifuged, and pellets were washed with RPMI 1640 to remove residues of 7H9 media containing malachite green. Pellets were resuspended in RPMI 1640 with 10% FBS, and clumping was disrupted by repeated passage through a 25G needle. Media were removed from THP-1 cells and replaced with media containing H37Ra at a multiplicity of infection of 5 for 4 h. THP-1 cells were washed two times with RPMI 1640 after 4 h to remove extracellular bacteria, followed by a 24-h incubation in RPMI 1640 with 10% FBS containing vehicle (DMSO), kynurenine (Sigma; final concentration 50  $\mu$ M in DMSO), or indirubin (Sigma; final concentration 20  $\mu$ M in DMSO). For Trp supplementation, Trp powder was added directly to 10% FBS-containing RPMI 1640 in a 50-ml Falcon tube on a rotating shaker for 30 min at room temperature, and then passed through a 0.2- $\mu$ m filter.

### Small interfering RNA-mediated knockdown

One day after PMA-induced THP-1 differentiation, small interfering RNAs (siRNAs) targeting *AHR* and the nontargeting scrambled control were transfected into THP-1 cells using PepMute reagent (SigmaGen; cat #SL100566), according to the manufacturer's instructions. After 24 h, media were replaced with RPMI 1640 with 10% FBS. Then, cells were infected with H37Ra. The following siRNA sequences were used for knockdown: negative control siRNA (nonsilencing; QIAGEN; SI03650325); Hs *AHR*\_6 Flexi Tube siRNA (QIAGEN; SI03043971) 5'-CGGCAUA-GAGACCGACUUAATT-3'; SMART pool ON-TARGET plus human *AHR* (196) siRNA (Dharmacon; L-004990-00-0005) 5'-GCAAGUUAUUGGC-AUGUUU.GAACUCAAGCUGUAUGGUA-3', 5'-GCACGAGAGGCUCA-GGUUA.GCAACAAGAUGAGUCUAUU-3'; SMART pool ON-TARGET plus mouse *Ahr* (11622) siRNA (Dharmacon; L-044066-00-0005) 5'-CAAGGGAGGUUAAAGUAUC-3', 5'-UCAGAGCUCUUCCGGAUA-3', 5'-GUGCAGAGUUGAGGUGUUU-3', 5'-CGACAUACGGACGAAUC-3'; and ON-TARGET plus nontargeting siRNAs (Dharmacon; D-001810-0X, Species H, M, R).



### Macrophage CFU assays

At the indicated time points, cells were lysed with PBS containing 0.03% Triton X-100, resuspended, and plated in serial dilution and triplicates for day 3 or day 5 time points using an inoculating turntable (Sensorturn pro) on Middlebrooks 7H10 Agar (Difco) containing 10% oleic acid, albumin, dextrose complex (BD Biosciences). To check for clumping, mycobacteria were directly stained, mounted with Prolong Gold (Life Technologies) containing DAPI on a slide, covered by a coverslip, and imaged with a fluorescence bright-field microscope (Axiovert; Zeiss) at 100 $\times$  magnification (Supplemental Fig. 1; the images are representative of 20 images total).

### Western blot analysis and Abs

Protein extracts from cells were prepared in lysis buffer (0.5% Nonidet P-40, 0.5 mM EDTA, 20 mM Tris [pH 7.6], 100 mM NaCl, Sigma protease inhibitor mixture), sonicated for 10 s for two cycles, amplitude 30% on the Vibra-Cell SONICS system, and centrifuged at 10,000 rpm for 10 min. Protein concentration was determined using Bio-Rad DC Protein assay. The normalized protein samples were loaded on Precast Bio-Rad Mini-TGX 4–15% polyacrylamide gel (456-1084). The following Abs, verified by siRNA knockdown, were used: AHR Ab (sc-5579; Santa Cruz), IDO (12006; Cell Signaling), TDO2 (H00006999-D01P; Abnova), ARNT H-172 (sc-5580; Santa Cruz), RELB C-19 (sc-226; Santa Cruz), and normal rabbit IgG (2729; Cell Signaling); H3K4 monomethylation (H3K4me1) chromatin immunoprecipitation (ChIP) grade Ab was used for ChIP-sequencing (ChIP-seq) (ab8895; Abcam).

### ChIP assays

Infected and uninfected PMA-differentiated THP-1 cells were collected 24 h postinfection. Cells were fixed by adding formaldehyde directly to the medium to a final concentration of 1%, followed by incubation for 20 min at room temperature and quenching with 125 mM glycine. Cells were scraped, and the cell pellet was washed once with cold PBS containing 125 mM glycine and washed three times with cold PBS. The cell pellet was sonicated in lysis buffer (5 mM PIPES [pH 8.5], 85 mM KCl, 1% [v/v] IGEPAL CA-630, 50 mM NaF, 1 mM PMSF, 1 mM phenylarsine oxide, 5 mM sodium orthovanadate, and additional inhibitors). Nuclear pellets were dissolved in 500  $\mu$ l nuclei-lysis buffer (50 mM Tris-HCl [pH 8], 10 mM EDTA, 1% [w/v] SDS, 50 mM NaF, 1 mM PMSF, 1 mM phenylarsine oxide, 5 mM sodium orthovanadate, and additional inhibitors) and incubated for 15 min on ice. Lysates were sonicated on a Bioruptor with a repeated cycle of 10 s on and 20 s off for 15 cycles, five times, resulting in DNA fragments of 200–600 bp. Cellular debris was removed by centrifugation. A total of 50  $\mu$ l of the lysate was diluted 1:10 in ChIP dilution buffer, 5  $\mu$ g Ab or nonspecific rabbit IgG was added, and the samples were incubated overnight at 4°C on a rotating platform. The immune complexes were collected using 40  $\mu$ l Protein A Beads for 2 h at 4°C with rotation. The beads were washed for 4 min on a rotating platform, as previously described (25), and the immune complexes were eluted twice using 200  $\mu$ l elution buffer (1% SDS, 100 mM NaHCO<sub>3</sub>). The supernatants were combined, and the immune complexes were reverse cross-linked for 6 h at 65°C in the presence of proteinase K (20 mM). DNA was purified using the MinElute PCR Purification Kit (QIAGEN). ChIP primers are listed in Supplemental Table I. Quantification of immunoprecipitated material was performed by quantitative PCR (qPCR). The same ChIP protocol as above was used for ChIP-seq, followed by library preparation using the TruSeq Library Kit (Illumina), according to the manufacturer's recommendations. DNA libraries for each immunoprecipitation (IP) and mock IP (a.k.a. input) were sequenced on an Illumina HiSeq sequencer, obtaining an average of 60 million reads/sample using 100-base-long reads and ~300 bases insert size. Reads were mapped to the human genome (hg19) with BWA 0.5.9-r16 (26, 27), using default settings, and converted to BAM files with SAMtools (28, 29). For each experiment, ChIP-seq peaks were obtained by comparing the read from the IP with that from mock IP and calling peaks, using MACS 1.4.2 (27), with a fold change  $\geq$  2 and 5% false discovery rate. BED files were annotated and filtered using SnpEff (26) and SnpSift (29). The data have been submitted to Array Express under accession number E-MTAB-3192 (<http://www.ebi.ac.uk/arrayexpress/experiments/E-MTAB-3192/>).

### RNA extraction

To maximize RNA yields and purity, the following modified protocol was used. RNA extraction was initially performed using TRIzol reagent (Invitrogen) or Tri-Reagent (Favorgen). After adding chloroform and centrifugation at 12,000 rpm for 15 min at 4°C, supernatant was passed through the first column of a Blood/Cultured Cell Total RNA Mini Kit (FABRK 001; Favorgen), mixed with the same volume of 75% ethanol,

and passed through the RNA extraction column (second column, red) of the Cultured Cell Total RNA Mini Kit. The column was washed and eluted according to the manufacturer's instructions. All centrifugation steps were done at 14,000 rpm.

### Reverse transcription/qPCR

Reverse transcription (RT) was performed with a Bio-Rad iScript cDNA Synthesis Kit (cat. no. 170-8891), and qPCR was performed with SsoFast EvaGreen Supermix (cat. no. 172-5211) on an Illumina Eco qPCR cyclor (polymerase activation, 95°C, 10 min, followed by 45 cycles of 95°C, 10 s denaturation; 60°C, 30 s annealing/elongation). Expression was normalized to *ACTB* and *RN18S1* for human THP-1 cells and *Hmbs* for mouse cells. Primers are listed in Supplemental Table I.

### Microarray analysis

Cells were transfected with anti-AHR siRNA (QIAGEN; SI03043971) and negative control siRNA (nonsilencing; QIAGEN; SI03650325) for 24 h. Controls cells or cells were infected with H37Ra (multiplicity of infection = 5) for 4 h and washed twice. Twenty-four hours later, host RNA was extracted using an RNeasy Plus Mini Kit (QIAGEN; 74134) by centrifugation at 14,000 rpm. The mean RNA integrity number of RNAs, as assessed by an Agilent 2100 Bioanalyzer, was 9.66. Microarray analysis was performed at the McGill University and Genome Quebec Innovation Centre, and Human Gene 2.0 ST arrays (Affymetrix) were probed with samples from two independent experiments, each performed in quadruplicate. Results of microarray analysis have been submitted to the National Center for Biotechnology Information Gene Expression Omnibus under accession number GSE70200 (<http://www.ncbi.nlm.nih.gov/geo/query/acc.cgi?acc=GSE70200>).

### Secreted cytokine and chemokine quantification

Culture medium supernatants of THP-1 cells were collected 24 h postinfection with H37Ra. Following a centrifugation step at 6000 rpm for 5 min and filtration through a 0.2- $\mu$ m filter, the supernatant samples were sent to Eve Technologies or Quansys Biosciences for Milliplex or BioPlex analysis, respectively. Based on the sample preparation manual, ethanol was used as carrier instead of DMSO for Milliplex and BioPlex analyses, because DMSO can negatively affect multiplex assays.

### Statistical analysis

All experiments are representative of three to five biological replicates. Statistical analysis was conducted using SYSTAT13 Trial by performing one-way ANOVA, followed by the Tukey test for multiple comparisons.

## Results

### Elevated expression of several enzymes catalyzing Trp metabolism in *M. tuberculosis*-infected macrophages

Our expression-profiling studies in THP-1 macrophage-like cells revealed that infection with virulent or attenuated strains of *M. tuberculosis* (H37Rv or H37Ra, respectively) induced very similar and widespread patterns of transcriptional reprogramming within 24 h (25). The most highly induced genes in infected THP-1 cells included, not surprisingly, those encoding several cytokines and other factors implicated in intracellular signaling. However, the list also contained *IDO1* and *TDO2*, whose expression was similarly induced ~50-fold after 24 h in either H37Ra- or H37Rv-infected THP-1 cells (Supplemental Fig. 2A). Upregulation of *TDO2* and *IDO1* was reproduced by RT/qPCR in both H37Ra-infected THP-1 cells and in infected primary human macrophages (Fig. 1A, 1B), and elevated expression of the encoded proteins in infected THP-1 cells and primary macrophages was confirmed by Western blotting (Fig. 1C–E). Moreover, an extended time course revealed that levels of *TDO2* and *IDO1* continued to rise sharply through  $\geq$ 48 h of infection in THP-1 cells (Supplemental Fig. 2B, 2C). *TDO2* and *IDO1* catalyze the rate-limiting step of Trp catabolism to kynurenines (Fig. 1A), which produces ligands for AHR (4, 5). Pathways mapping of microarray data revealed that infection also enhanced expression of downstream enzymes metabolizing kynurenines, including kynurenine monooxygenase and kynureninase, which catalyze the conversion of the Trp me-

tabolite L-formylkynurenine to 3-hydroxyanthranilic acid (HAA; Fig. 1F, Supplemental Fig. 2D). Regulation of these genes during infection was confirmed by RT/qPCR in THP-1 cells and primary macrophages (Fig. 1G, 1H). Other work showed that IL-17 production from Th17 cells could be controlled in vitro by addition of individual or mixed Trp/kynurenine metabolites, with HAA being the most potent (30). In contrast, although *IDO1* and *TDO2* expression was strongly induced, infection with either strain had little effect on the levels of related *IDO2* (Supplemental Fig. 2D).

#### Engagement of AHR signaling during *M. tuberculosis* infection

Because metabolism of Trp along the kynurenine pathway induces AHR signaling, we determined the expression levels of the receptor and its heterodimeric partners ARNT and RELB in uninfected and infected THP-1 cells. Analysis of the microarray data revealed that *AHR*, *ARNT*, and *RELB* transcripts were well expressed in both uninfected and infected cells (25). Expression of *AHR* and *RELB* in THP-1 cells was enhanced modestly (1.5–2-fold) and 3–4-fold, respectively, after 24 h of infection with either H37Ra or H37Rv, whereas that of *ARNT* was slightly inhibited (25) (Supplemental Fig. 2E). These results were verified by RT/qPCR in uninfected and H37Ra-infected THP-1 cells, which revealed that *AHR* and *RELB* expression was elevated through  $\geq 48$  h of infection (Fig. 2A, Supplemental Fig. 2F, 2G). Essentially identical results were obtained in infected primary human macrophages: the *AHR* gene was robustly expressed and further induced  $\sim 3$ -fold after 24 h of infection. Similarly, expression of *RELB* was enhanced 3-fold in

infected primary cells (Fig. 2B). Infection led to a substantial increase in both AHR and RELB protein expression within 24 h in infected THP-1 cells (Fig. 2C). Taken together, the above results suggest that AHR signaling may be induced upon H37Rv or H37Ra infection. We analyzed DNA binding of AHR and its heterodimeric partners, by ChIP assay in infected THP-1 cells, to three confirmed or putative target genes, *IL10*, *IL8* (*CXCL8*), and *IL1B*, all of which are induced (Fig. 2D). ChIP analysis revealed that infection enhanced binding of AHR and ARNT to AHRE (31) in the *IL10* promoter (Fig. 2E) in THP-1 cells. Similarly, elevated AHR and RELB binding was observed, in infected THP-1 cells, to the composite element (32) in the *IL8* promoter (Fig. 2F).

Previous studies showed that *IL1B* is also induced by *M. tuberculosis* infection of primary human macrophages (25), a result that we confirmed in this study (Supplemental Fig. 2H). Moreover, other work suggested that AHR antagonism inhibits *IL1B* expression (33). Therefore, we screened for potential AHREs in the *IL1B* gene. This revealed a sequence located  $\sim 8.5$  kb upstream of the gene and an intragenic motif. Both of these motifs bound AHR and ARNT robustly, and binding of both heterodimeric partners was elevated in infected cells (Fig. 2G). Next, we tested the effects of AHR ablation on the expression of *IL1B*, as well as *IL8*, in THP-1 cells. Transient expression of AHR-specific siRNAs led to complete loss of AHR protein (Fig. 3A). Importantly, *IL1B* and *IL8* expression was strongly attenuated by depletion of AHR (Fig. 3B). In agreement with these findings, AHR antagonist CH223191 largely blocked induction of *IL1B* and *IL8* expression in H37Ra-

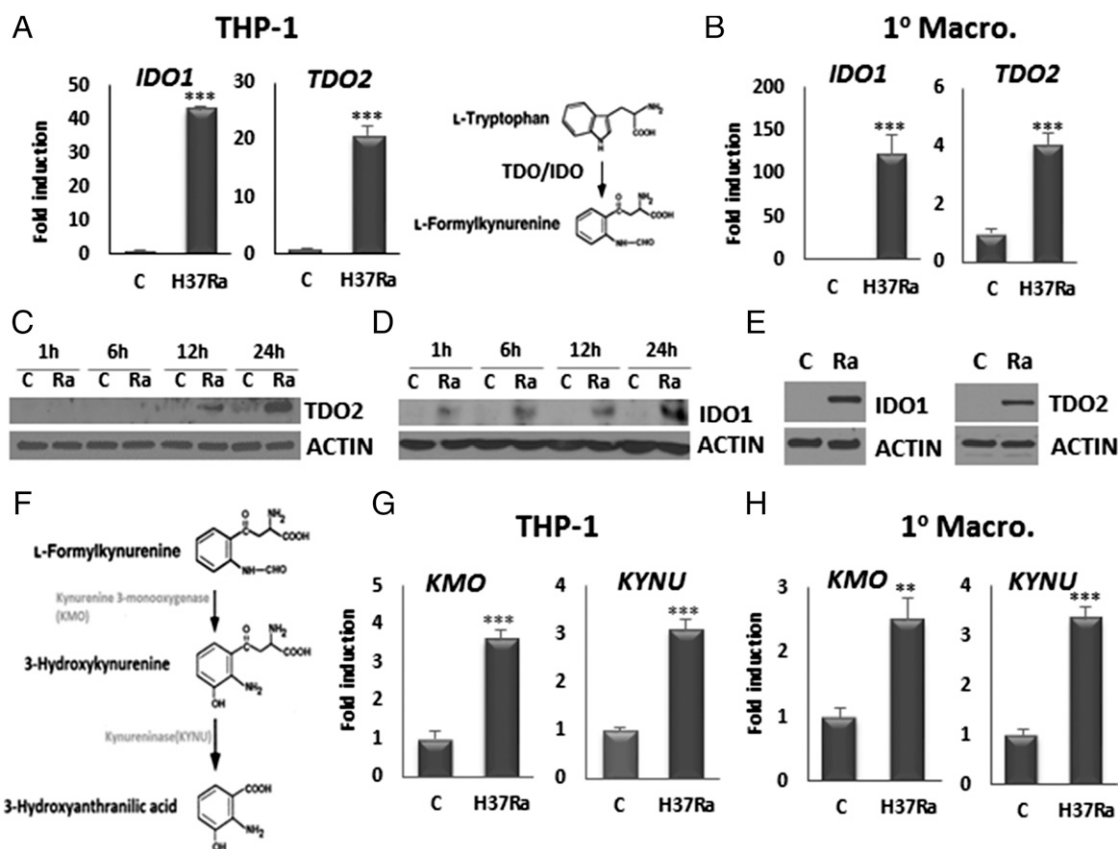


**FIGURE 1.** Elevated expression of Trp-metabolizing enzymes in *M. tuberculosis*-infected macrophages. Analysis of *IDO1* and *TDO2* expression after 24 h of infection of THP-1 cells (A) or primary human macrophages (B) with H37Ra by RT/qPCR. (A) Schematic representation of the catabolism of Trp to L-formylkynurenine by TDO/IDO enzymes (right panel). Analysis of TDO2 (C) and IDO1 (D) protein expression by Western blotting in H37Ra-infected THP-1 cells. (E) Analysis of TDO2 and IDO1 protein expression by Western blotting in control and H37Ra-infected (24 h) primary human macrophages. Analysis of the expression of genes encoding downstream enzymes of the kynurenine pathway kynurenine 3-monooxygenase (KMO) and kynureninase (KYNU) (F) in THP-1 cells (G) and primary human macrophages (H) infected with vehicle or H37Ra for 24 h. Representative results of multiple biological replicates are presented. \*\* $p \leq 0.01$ , \*\*\* $p \leq 0.001$ , one-way ANOVA followed by the Tukey post hoc test for multiple comparisons.

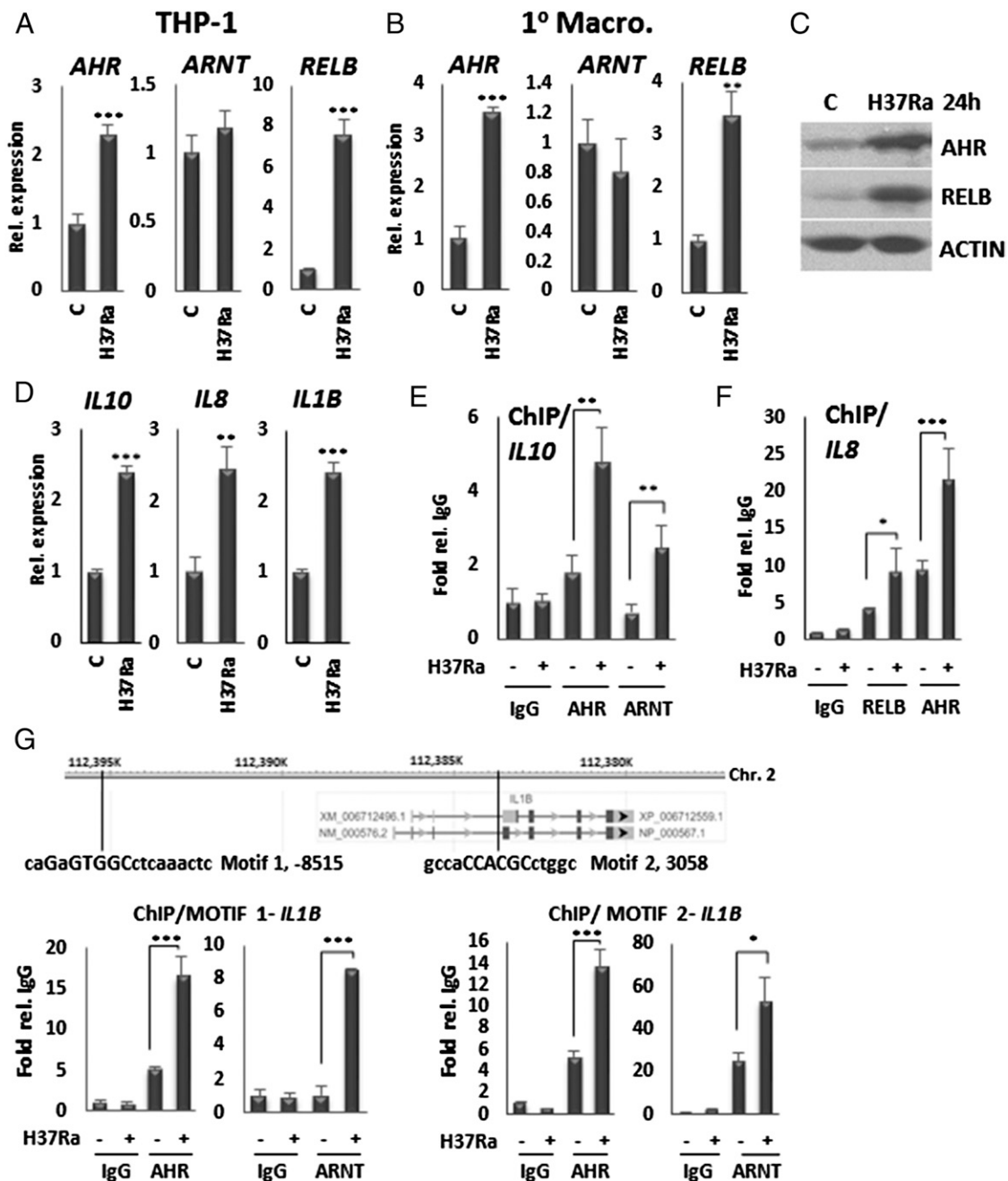


**FIGURE 2.** Expression and DNA binding of AHR and heterodimeric partners ARNT and RELB in uninfected and infected macrophages. **(A)** RT/qPCR analysis of *AHR*, *ARNT*, and *RELB* expression after 24 h of H37Ra infection in THP-1 cells. **(B)** RT/qPCR analysis of *AHR*, *ARNT*, and *RELB* expression after 24 h of H37Ra infection in primary human macrophages. **(C)** Analysis of the effect of 24 h of H37Ra infection of THP-1 cells on the expression of AHR and RELB proteins by Western blotting. **(D)** Expression of AHR target genes *IL1B*, *IL10*, and *IL8* in uninfected THP-1 cells and cells infected with H37Ra for 24 h. **(E)** ChIP analysis of AHR and ARNT binding to the promoter of AHR target gene *IL10* in uninfected and H37Ra-infected (24 h) THP-1 cells. **(F)** ChIP analysis of AHR and RELB binding to the composite element of the *IL8* promoter in uninfected and H37Ra-infected (24 h) THP-1 cells. **(G)** Identification and characterization by ChIP assay of elements binding AHR and ARNT in the promoter of the *IL1B* gene. A schematic representation of the *IL1B* gene is shown (upper panel). Representative results of multiple biological replicates are presented. \* $p \leq 0.05$ , \*\* $p \leq 0.01$ , \*\*\* $p \leq 0.001$ , one-way ANOVA followed by the Tukey post hoc test for multiple comparisons.

infected cells (Fig. 3C). We probed further the potential role of Trp metabolism in driving AHR signaling in infected THP-1 cells and found that exogenous kynurenine increased expression of *IL1B* and *IL8* in infected cells (Fig. 4A, 4B). Taken together, these data strongly support the hypothesis that elevated Trp metabolism contributes to enhanced AHR signaling in infected THP-1 cells. Importantly, exogenous Trp led to a dose-dependent reduction in *M. tuberculosis* burden (Fig. 4C). Exogenous kynurenine (Fig. 4D), or the synthetic AHR agonist indirubin (Fig. 4E), also

reduced mycobacterial burden in infected THP-1 cells to a similar degree as added Trp. Taken together, the above experiments are consistent with enhanced AHR signaling induced by Trp metabolism acting to inhibit *M. tuberculosis* growth.

#### Contribution of AHR signaling to immune responses in infected cells

To develop a broader picture of the role of AHR signaling in host macrophage responses to *M. tuberculosis* infection, we probed

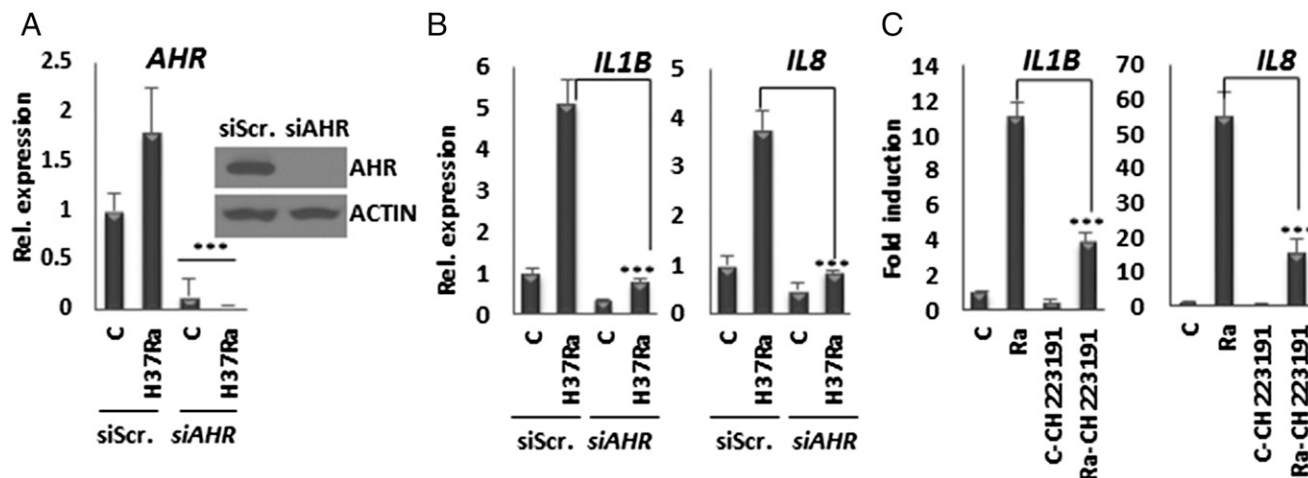


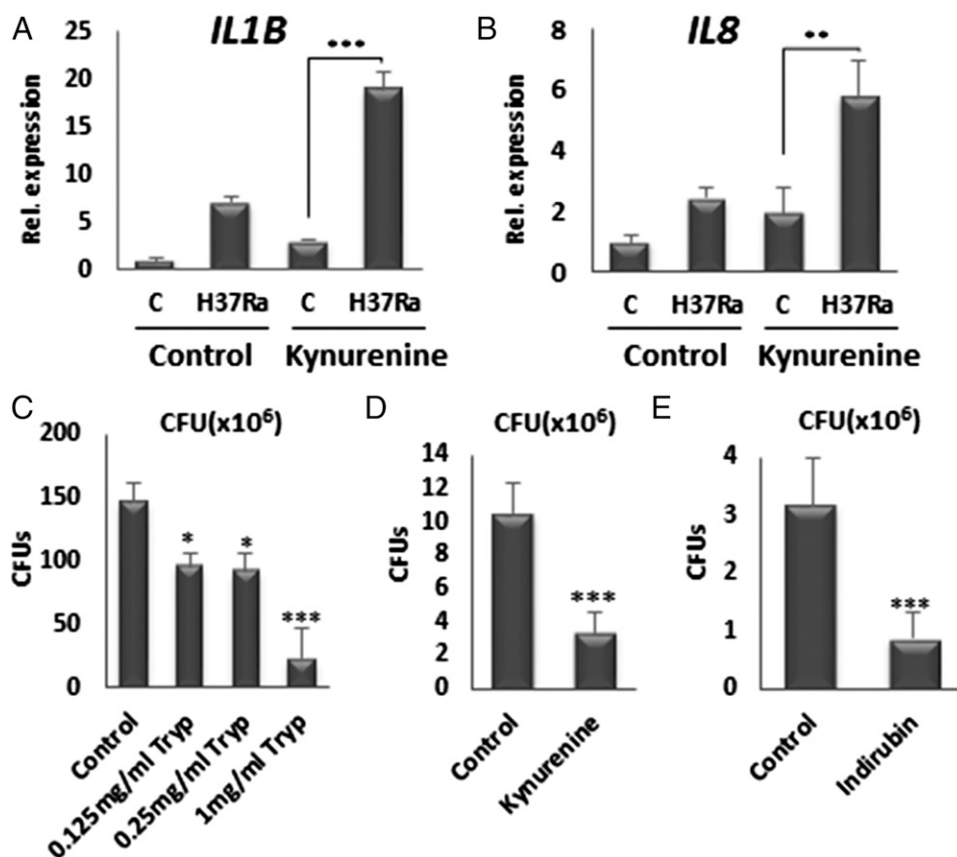
**FIGURE 3.** AHR-dependent regulation of target genes in uninfected and infected THP-1 cells. **(A)** Effect of scrambled or AHR-specific siRNAs on expression of AHR transcripts and protein in uninfected and infected THP-1 cells. Western blot of AHR expression (*inset*). **(B)** Effect of scrambled and AHR-specific siRNAs on the expression of *IL1B* and *IL8* transcripts in uninfected and infected THP-1 cells. **(C)** AHR antagonist suppresses *IL1B* and *IL8* mRNA expression in H37Ra-infected THP-1 cells. Representative results of multiple biological replicates are presented. \*\*\* $p \leq 0.001$ , one-way ANOVA followed by the Tukey post hoc test for multiple comparisons.

Affymetrix Human 2.0ST microarrays with cDNA derived from infected THP-1 macrophages transfected with scrambled or AHR-specific siRNAs. Transfections, performed in quadruplicate with specific siRNAs, led to ~90% knockdown of AHR transcripts (Fig. 5A), a degree of depletion that leads to complete loss of AHR protein (Fig. 3A). Importantly, microarray analysis revealed that depletion of AHR in infected THP-1 cells attenuated the expression of control genes *IL1B*, *IL10*, and *IL8*. In addition, expression of *PTGS2* (*COX-2*) and *PTGES* (PG E synthase) transcripts, along with those encoding effectors of *PTGS2* gene

expression, were reduced by AHR ablation (Supplemental Fig. 3A), in agreement with previous observations that expression of *PTGS2* and *PTGES* in lung fibroblasts is AHR dependent (34). Notably, expression levels of *IDO1* and *IDO2*, as well as *TDO*, were also lower in AHR-deficient THP-1 cells, consistent with previous studies showing that dioxin-stimulated AHR signaling induced *IDO1* and *IDO2* expression (35) and with the induction of a positive-feedback loop maintaining elevated AHR signaling.

In total, the expression of 420 genes was altered in AHR-depleted THP-1 cells, using the relatively stringent cut-off of

**FIGURE 4.** Probing the relationship between Trp metabolism and AHR target gene regulation. Analysis of the effect of exogenous kynurenine (50  $\mu$ M) on the expression of AHR target genes *IL1B* (A) and *IL8* (B) in uninfected and H37Ra-infected THP-1 cells. **(C)** Effects of increasing concentrations of exogenous Trp on mycobacterial burden in *M. tuberculosis*-infected THP-1 cells 5 d postinfection. **(D)** Effects of exogenous kynurenine (50  $\mu$ M) on mycobacterial burden after 5 d of infection of THP-1 cells with H37Ra. **(E)** Effects of synthetic AHR agonist indirubin (20  $\mu$ M) on mycobacterial burden after 5 d of infection of THP-1 cells with H37Ra. Representative results of multiple biological replicates are presented in (A) and (B), whereas cumulative results of three biological replicates are presented in (C)–(E). \* $p \leq 0.05$ , \*\* $p \leq 0.01$ , \*\*\* $p \leq 0.001$ , one-way ANOVA followed by the Tukey post hoc test for multiple comparisons.





2-fold change in expression, and downregulated transcripts outnumbered upregulated genes by almost 3:1. The data provide evidence that AHR signaling contributes to the expression of a number of genes encoding IL subunits and chemokines (Table I). Including *IL1B*, *IL10*, and *IL8* (Supplemental Fig. 3B), we verified the effect of AHR ablation on the expression of 10 genes in infected THP-1 cells, all of which were in qualitative agreement with the results of the microarray analysis (Fig. 5B). These included *CCL1*, a previously identified TB susceptibility locus (36), *CXCL1*, which encodes a neutrophil chemokine highly induced during mycobacterial infection (37), and *CXCL14*, encoding a dendritic cell chemokine with purported antimicrobial peptide activity (38, 39). We further analyzed the effect of blocking AHR signaling in infected THP-1 cells on cytokine production by screening for the secretion of a panel of cytokines (Milliplex; Eve Technologies); this revealed that treatment of cells inhibited se-

cretion of a number of cytokines, including IL-1 $\beta$ , IL-10, CXCL1, and CCL1 (Fig. 5C), in agreement with our gene expression studies.

We also confirmed the reduced expression, in AHR-depleted THP-1 cells, of three genes encoding calcium binding proteins with antimicrobial activity: S100A8, A100A9, and S100A12 (40, 41) (Supplemental Fig. 3C). Indeed, bioinformatic analysis of disease processes and signaling pathways confirmed that AHR depletion altered the expression of numerous genes implicated in immune responses to infection, as well as cancer (Fig. 5D, 5E). Intriguingly, the list of downregulated genes and the cytokines whose secretion was inhibited by blocking AHR signaling included both subunits of IL-23 [*IL23A* and *IL12B* (IL-12 p40)] (Fig. 5B, 5C, Table I). Reduced expression of IL-23 in the absence of AHR is of considerable interest because it is a macrophage-derived cytokine (42) that is required for long-term control of

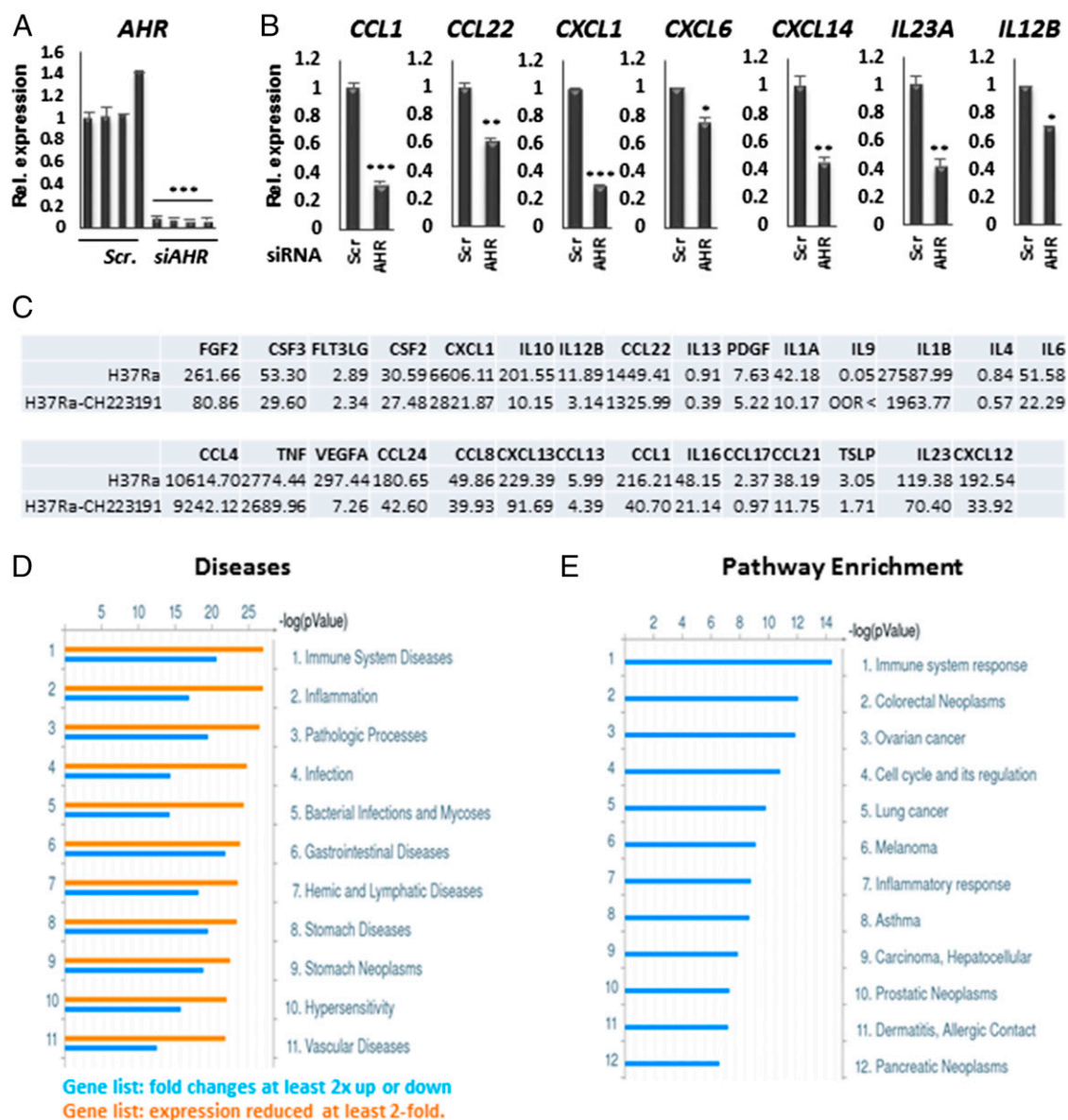


**FIGURE 5.** Comparative gene expression profiling in control and AHR-depleted H37Ra-infected THP-1 cells. **(A)** RT/qPCR analysis of *AHR* gene expression in the quadruplicate control and *AHR*-depleted samples used for microarray analysis. **(B)** Validation by RT/qPCR of the results of microarray analysis showing that AHR depletion leads to reduced expression of genes encoding chemokines and cytokines (see also Table I). **(C)** Profiles of cytokines secreted from H37Ra-infected THP-1 cells (24 h) treated with vehicle or AHR antagonist CH223191. **(D)** Bioinformatic analysis [MetaCore (69)] of all genes differentially expressed (at least 2-fold) or genes whose expression was downregulated only in AHR-depleted THP-1 cells. **(E)** Pathways mapping of all differentially regulated genes. \* $p \leq 0.05$ , \*\* $p \leq 0.01$ , \*\*\* $p \leq 0.001$ , one-way ANOVA followed by the Tukey post hoc test for multiple comparisons.



Table I. Genes encoding cytokines or cytokine subunits

	Name	Fold Change	p Value
NM_005755	EBI3	-6.88858	8.80E-10
NM_016584	IL23A	-6.01187	1.27E-08
ENST00000219235	CCL22	-5.80701	5.92E-06
NM_004887	CXCL14	-4.14662	1.37E-07
ENST00000222902	CCL24	-3.83993	0.000564
NM_002981	CCL1	-3.75812	0.005984
NM_000584	IL8	-3.05519	7.23E-08
NM_000575	IL1A	-2.99957	3.68E-06
NM_014438	IL36B	-2.78985	4.96E-06
NM_002416	CXCL9	-2.7	8.72E-06
ENST00000263341	IL1B	-2.52849	0.001197
ENST00000231228	IL12B	-2.45086	1.74E-06
NM_002993	CXCL6	-2.39968	0.000656
NM_001511	CXCL1	-2.3772	0.000887
NM_006274	CCL19	-2.04403	2.39E-05
NM_000572	IL10	-2.00943	0.000515

Data are taken from datasets for GSE70200 submitted to the Gene Expression Omnibus.

*M. tuberculosis* infection in the lung (22–24). Moreover, IL-23 secreted from macrophages drives differentiation of IL-22-producing ILCs and NK cells in the gut and lungs (42–44), and *IL22* is a direct AHR target gene in those cells. Taken together, these data suggest that, in addition to its established role in controlling IL-22 synthesis in NK cells and ILCs (11, 12), AHR signaling may function upstream to induce IL-23 production by macrophages.

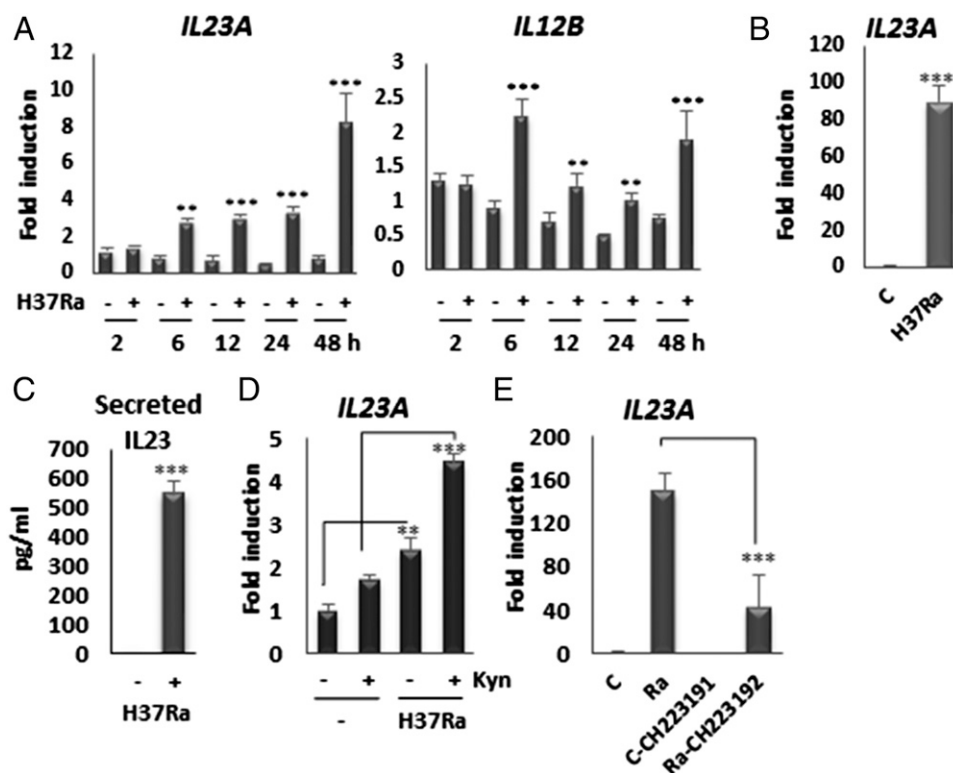
#### IL23A is a direct AHR target gene

Given the potential role of IL-23 as a key effector of AHR signaling and the fact that the IL-23A subunit controls the specificity of the cytokine, we were interested in determining whether *IL23A* gene expression was directly regulated by the receptor. A time-course analysis revealed that *IL23A* transcript levels rose during infection of THP-1 cells, particularly between 6 and 48 h (Fig. 6A), a profile

reminiscent of those for the *IDO1* and *TDO2* genes. *IL12B* expression was elevated in *M. tuberculosis*-infected THP-1 cells, although not to the same degree as that of *IL23A* (Fig. 6A). We also observed a strong induction of *IL23A* expression after 24 h of infection in primary human macrophages (Fig. 6B). In agreement with these findings, IL-23 secretion, which was below the limit of detection in uninfected THP-1 cells, was strongly enhanced by *M. tuberculosis* infection (Fig. 6C). The strong dependence of IL-23 secretion on infection is consistent with a previous report showing that its release is regulated by the maturation and secretion of IL-1 $\beta$  (45), which is also triggered by *M. tuberculosis* infection (25). Consistent with a potential role for AHR in directly regulating its transcription, exogenous kynurenine significantly enhanced *IL23A* mRNA expression in THP-1 cells (Fig. 6D) in a pattern similar to that of the target genes *IL1B* and *IL8* (Fig. 4A, 4B), whereas incubation with AHR antagonist CH223191 strongly attenuated this induction (Fig. 6E).

The *IL23A* locus is compact, located on chromosome 12, and flanked by the *STAT2* and *PAN2* genes (Fig. 7A). Our ChIP-seq analysis of markers for transcriptional enhancers in macrophages revealed the presence, in both uninfected and infected THP-1 cells, of an extended region encompassing the *IL23A* locus of elevated H3K4me1 (Fig. 7A). H3K4me1 is an epigenetic mark associated with poised or active enhancers (46–49). In addition, analysis of ChIP-seq data derived from seven cell lines generated by the ENCODE project (50) revealed the presence of several peaks within this region corresponding to elevated H3K27 acetylation (H3K27Ac, Fig. 7A), a mark associated with active transcriptional enhancers (46, 49). Taken together, these data strongly suggest that the region directly upstream of the *IL23A* transcription start site contains transcriptional enhancer(s). AHREs are generally defined as containing the core motif GCGTG within an extended consensus sequence 5'-T/GNGCGTGA/CG/CA-3' (51). We screened between the *PAN2* and *IL23A* loci for sequences with homology to extended core AHRE motifs (Fig. 7A). This revealed three potential elements lying 3675, 2025, and 1375 bp upstream of the *IL23A*

**FIGURE 6.** Regulation of *IL23A* in *M. tuberculosis*-infected macrophages. (A) Analysis by RT/qPCR of the expression of the genes encoding IL-23 subunits *IL23A* and *IL12B* over a 48-h time course in control and H37Ra-infected THP-1 cells. (B) Induction by RT/qPCR of *IL23A* mRNA expression in primary human macrophages after 24 h of infection with H37Ra. (C) Analysis of IL-23 secretion from uninfected and infected macrophages. (D) Effect of exogenous kynurenine (50  $\mu$ M) on the expression of *IL23A* in uninfected and H37Ra-infected THP-1 cells. (E) Treatment with AHR antagonist CH223192 (100 nM) inhibits *IL23A* expression in *M. tuberculosis*-infected THP-1 cells. Representative results of multiple biological replicates are presented. \*\* $p \leq 0.01$ , \*\*\* $p \leq 0.001$ , one-way ANOVA followed by the Tukey post hoc test for multiple comparisons.



transcription start site, one of which (−2025) corresponds to an extended consensus sequence. ChIP experiments in THP-1 cells revealed that binding of AHR and its heterodimeric partners ARNT and RELB to these regions is markedly enhanced by infection (Fig. 7B–D), with, as expected, the strongest association of all three proteins observed at the extended consensus motif (−2025 bp, Fig. 7C). Notably, the extended consensus motif corresponds to a region of peak H3K27Ac, based on ENCODE data (Fig. 7A). These data reveal that the human *IL23A* gene is a direct target gene of AHR/ARNT heterodimers in humans.

One indicator of the physiological importance of a signal transduction pathway is the extent of its conservation throughout evolution. To further probe the regulation of *IL23A* expression by AHR, we analyzed the conservation of AHREs in primates and other species. As expected, there was almost complete conservation among human, chimpanzee, and rhesus sequences (Fig. 8A). Although the relative arrangement of the genes encoding *PAN2*, *IL-23A*, and *STAT2* were conserved in other species, the positions of the human/primate motifs are not conserved in mouse (Fig. 8A) or in rabbit or rat (data not shown). However, closer examination of the region between the mouse *Pan2* and *Il23a* genes revealed four putative near-consensus elements (Fig. 8B). We were able to design specific primers to amplify three of these regions (motifs 1, 3, and 4) in ChIP assays, which revealed strong AHR binding that was augmented on two of the three motifs by H37Ra infection of mouse macrophages (Fig. 8C). Furthermore, knockdown of *Ahr*

expression in infected mouse macrophages strongly diminished *Il23a* mRNA expression (Fig. 8D). Taken together, these results reveal that AHR signaling directly induces transcription of the gene encoding IL-23A in a variety of species (Fig. 9).

## Discussion

The studies described above reveal that expression of several components of the Trp/kynurenine metabolic pathway are strongly stimulated in *M. tuberculosis*-infected THP-1 cells and in primary human macrophages. In expression profiling studies, genes encoding the enzymes TDO2 and IDO1 were among the most highly induced within 24 h of infection with either virulent or attenuated strains of *M. tuberculosis* (Fig. 1). Notably, Trp metabolism via the IDO pathway is induced by IFNs during inflammatory responses, and it often occurs in concert with cytokine production associated with immune activation (5). Trp depletion in response to infection through induced TDO/IDO expression may be an effective strategy to reduce the viability of organisms such as *Chlamydia* and *Leishmania*, which are Trp auxotrophs; however, *M. tuberculosis* is capable of inducing Trp biosynthesis under stress conditions (52, 53), suggesting that induced Trp metabolism contributes to host responses to infection by other mechanisms. In addition to TDO2 and IDO1, infection stimulated expression of the *KMO* and *KYNU* genes, which encode enzymes that metabolize the TDO/IDO Trp metabolite L-formylkynurenine to HAA. Of individual or mixed Trp/kynurenine metabolites,

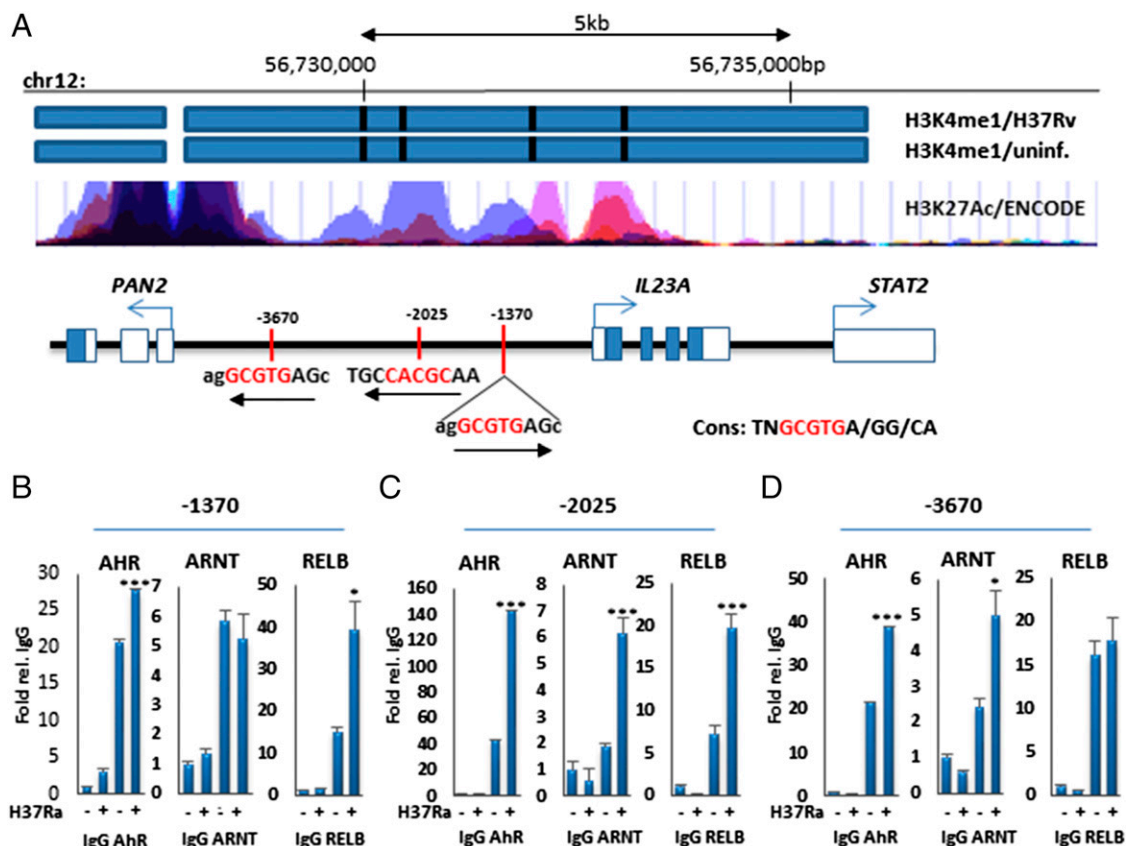
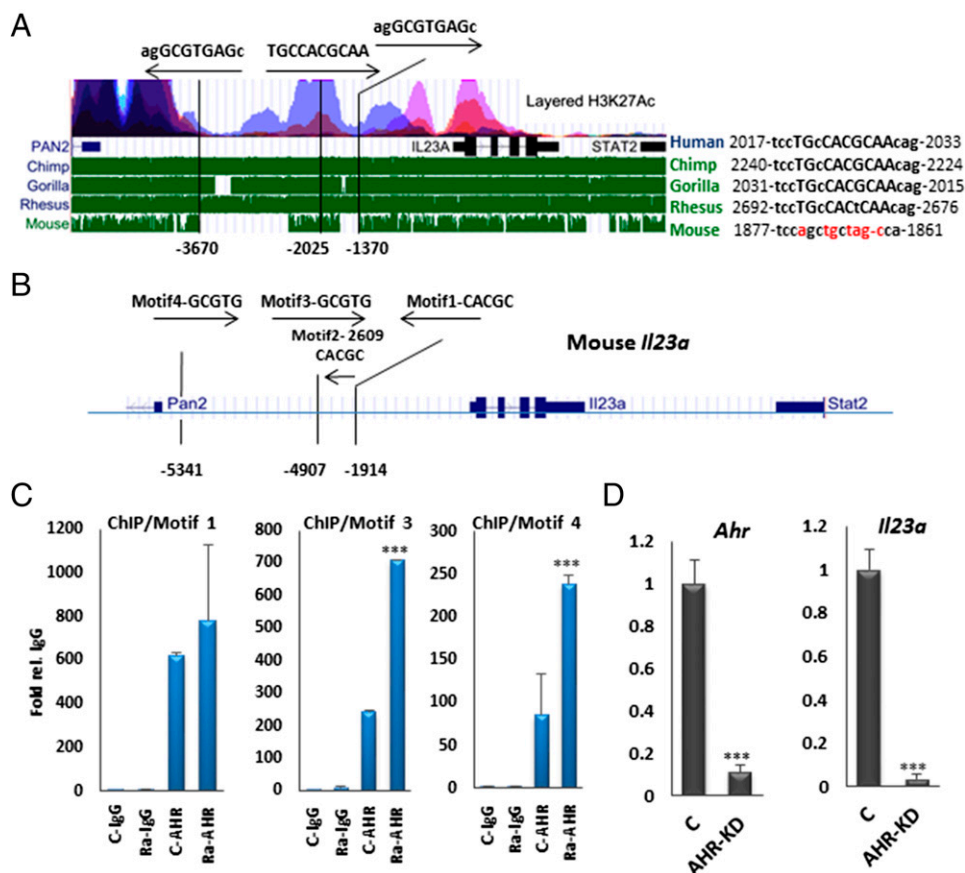


**FIGURE 7.** Identification of AHREs in the region of chromosome 12 containing the *IL23A* gene. **(A)** Horizontal bars delineate regions of elevated H3K4me1 in the region of the *IL23A* gene in uninfected (uninf.) and H37Rv-infected THP-1 cells, with peaks of monomethylation indicated by vertical black bars (top panel). Schematic representation of regions of elevated H3K27Ac determined in seven cell lines by the ENCODE consortium (middle panel). Schematic representation of the region containing the *IL23A* gene (note that only the 5' ends of the flanking *PAN2* and *STAT2* genes are shown) (bottom panel). The positions of motifs containing extended homology to the AHRE core GCGTG sequence (in red) are indicated. The extended consensus sequence is shown on the right. **(B–D)** Analysis of binding of AHR and its heterodimeric partners ARNT and RELB to upstream AHREs by ChIP assay in uninfected and infected THP-1 cells. Representative results of multiple biological replicates are presented. \* $p \leq 0.05$ , \*\*\* $p \leq 0.001$ , one-way ANOVA followed by the Tukey post hoc test for multiple comparisons.

**FIGURE 8.** Analysis of conservation of AHR regulation of *IL23A* gene expression. **(A)** Analysis of the conservation of putative AHREs in the human *IL23A* gene in primates and mouse. The human *PAN2-IL23A* region is shown, along with ENCODE H3K27Ac profiles and the position of putative AHREs (above). Regions of sequence conservation in primates and mouse are shown below, along with the conservation of the extended consensus AHRE (−2025 in the human genome). **(B)** Putative AHREs upstream of the mouse *Il23a* gene. **(C)** Analysis of AHR binding to putative AHREs by ChIP assay in uninfected and H37Ra-infected mouse macrophages. **(D)** Depletion of *Ahr* expression in *M. tuberculosis*-infected mouse primary macrophages inhibits *Il23a* gene expression, as analyzed by RT/qPCR. Representative results of multiple biological replicates are presented in (C) and (D). \*\*\* $p \leq 0.001$ , one-way ANOVA followed by the Tukey post hoc test for multiple comparisons.



HAA was the most potent at inhibiting Th17 cell differentiation (30). Similarly, HAA was the most potent of the kynurenine metabolites in assays of induction of AHR-dependent IL-22 production by T cells (54). HAA is a poor AHR ligand, but it readily undergoes nonenzymatic oxidative dimerization to cinnabaric acid, a tricyclic aromatic compound, which recent work showed is a potent AHR ligand that mimics the action of HAA in in vitro assays (54).

The gene regulatory events revealing induced Trp metabolism do not, in isolation, constitute definitive evidence that AHR signaling is elevated during infection. However, mRNA and protein expression of AHR and its heterodimeric partner RELB, but not ARNT, are also increased in infected cells, as is DNA binding of AHR heterodimerized with either RELB or ARNT to well-characterized target genes *IL10* and *IL8*. The elevated binding of ARNT (2–6-fold) to AHREs in the absence of changes in its expression is consistent with an upregulation of endogenous AHR agonist production. The ties between Trp metabolism and upregulated AHR signaling are reinforced by the observation that exogenous Trp, kynurenine, and unrelated AHR agonist indirubin produced similar reductions in mycobacterial burden. When this study was initiated there were no substantive links between AHR signaling and a role in the control of *M. tuberculosis* infection. However, recent work showed that resistance of *Ahr*-deficient mice to *M. tuberculosis* infection is reduced relative to their wild-type counterparts (17). Importantly, survival in total *Ahr*-knockout animals and mice deficient in the myeloid lineage only was reduced to an identical extent, revealing the importance of AHR signaling in myeloid cells in control of *M. tuberculosis* infection in this model (17). This study also provided evidence that molecules of mycobacterial origin could act as AHR agonists.

The reduction in mycobacterial burden in THP-1 cells treated with exogenous Trp, kynurenine, or indirubin observed in this study

is consistent with direct effects of AHR signaling within macrophages on *M. tuberculosis* viability. The gene expression profiling studies performed above revealed that AHR depletion disrupted the expression of numerous genes implicated in inflammation and immune responses to infection. Several of these included genes encoding cytokine/chemokines, with results substantiated by profiling cytokine/chemokine secretion from control infected cells or infected cells treated with an AHR antagonist. These results suggest that macrophage AHR signaling promotes immune responses to *M. tuberculosis* infection by inducing recruitment of other components of the immune system to sites of infection. Notably, exogenous kynurenine augmented, and *AHR* ablation in THP-1 cells reduced, the production of IL-1 $\beta$ , whose signaling is essential for survival in mouse models of *M. tuberculosis* infection (55, 56), and *IL8*, a neutrophil chemokine implicated in early responses to infection (57). We also characterized AHR binding sites in the *IL1B* gene; collectively, our results show that *IL1B* is a direct target gene of the receptor.

Intriguingly, expression of genes encoding both subunits of IL-23, *IL23A* and *IL12B*, was reduced in AHR-depleted cells, as was their secretion from AHR agonist-treated THP-1 cells. A direct role for AHR in control of IL-23 production is of interest for several reasons (Fig. 9); in humans, IL-23 and IL-1 $\beta$  induce the formation of Th17 cells expressing IL-17 subunits, IL-22, IFN- $\gamma$ , and the nuclear receptor ROR $\gamma$ t (58), a critical cell type for protection against *M. tuberculosis* infection (59). IL-23, rather than IL-12, with which it shares a common subunit, is the primary type 1 cytokine produced in mycobacterial infection (60), and IL-23 is required for long-term control of infection in mice (22). Mice deficient in the shared IL-12B (IL-12p40) subunit are more susceptible to TB than are animals lacking IL-12A (IL-12-specific IL-12p35 subunit) (61, 62). In humans, patients carrying muta-



tions in *IL23A* have yet to be identified; however, patients deficient in *IL-12B* displayed increased sensitivity to mycobacterial infection (61).

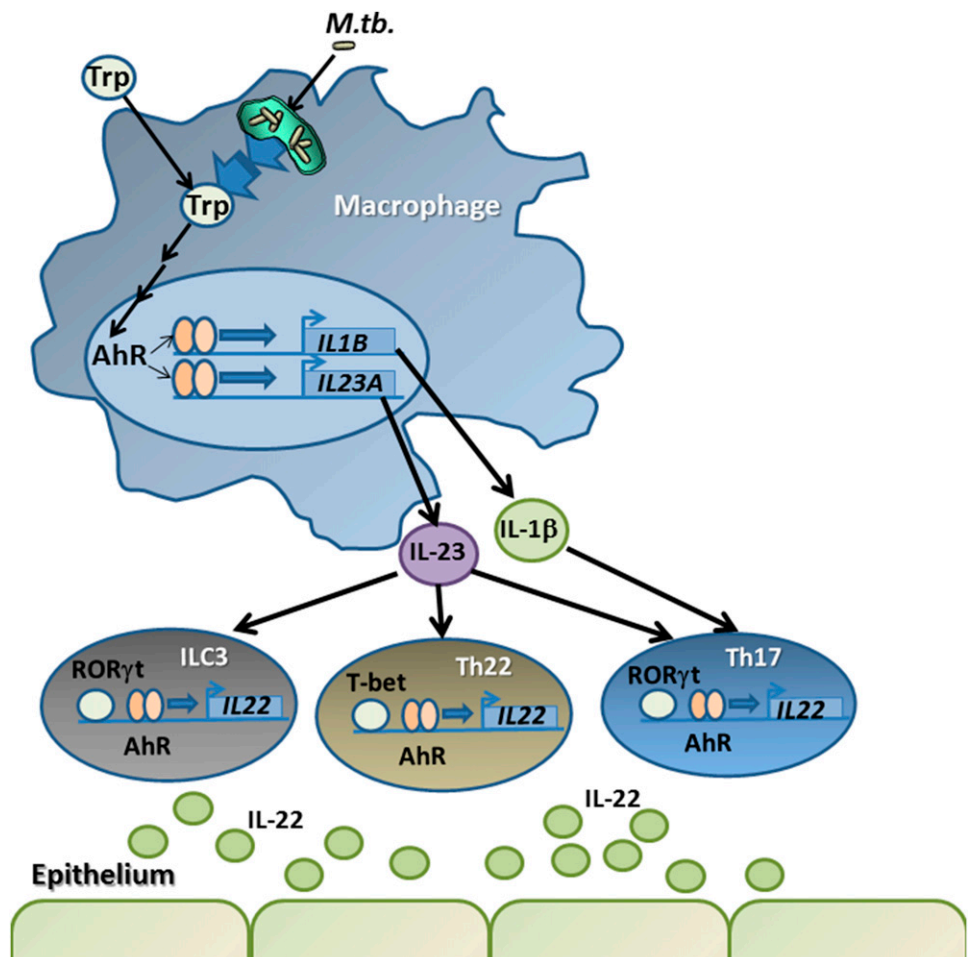
We found that *IL23A* expression was induced during the course of infection with a profile similar to that of the *TDO2* and *IDO1* genes. Our analysis of the H3K4me1 epigenetic mark in infected cells, coupled with the combined ChIP-seq studies of H3K27Ac by the ENCODE project (50), strongly suggested that the immediate upstream region of the relatively compact *IL23A* locus encompasses transcriptional enhancer(s). In humans, we found that this region contains three consensus or near-consensus AHREs, all of which were engaged at elevated levels by AHR and its heterodimeric partners in infected cells. Of these, the extended consensus sequence at  $-2025$  was found to be well conserved in primates but not in mice. However, other elements were characterized at similar positions in the mouse *Il23a* promoter. These data, along with observations that kynurenine enhances the expression of *IL23A* transcripts in human cells and that depletion of AHR has the opposite effect in human and mouse, strongly suggest that the gene is a direct target of AHR signaling in several species.

These and other results reveal that AHR drives an innate immune signaling cascade, starting with induced production of IL-1 $\beta$  and IL-23 in macrophages, which, in turn, leads to proliferation of IL-22-producing lymphoid cells and increased secretion of IL-22 (Fig. 9). IL-1 $\beta$  and its receptor, IL-1R1, are essential for survival in mouse models of *M. tuberculosis* infection (55, 56, 63). IL-1 signaling contributes to responses during early stages of infection, based on in vitro studies using macrophages from mice

deficient in IL-1A and IL-1 $\beta$  (64). Induction of IL-23 expression by AHR in macrophages is also relevant to responses to *M. tuberculosis*, because IL-23 production is required for long-term control of infection in the lung (22–24). Thus, loss of AHR-regulated production of IL-23 may contribute to the reduced survival of mice lacking AHR expression in the myeloid lineage (17). Moreover, mice lacking AHR are deficient in T cells producing IL-22 (2), an innate immune cytokine whose signaling stimulates epithelial tissue repair, elaboration of the mucosal layer, and production of antimicrobial peptides (65). IL-23 is essential for, or contributes to, the production of multiple T cell subtypes in which AHR signaling is implicated, including Th17, Th22, and ILC3 ILCs (12, 66, 67). In IL-22-producing Th17 and ILC3 cells, AHR cooperates with the nuclear receptor ROR $\gamma$ t to induce *IL22* gene transcription. AHR and ROR $\gamma$ t bind to upstream and intronic regulatory regions of the *IL22* gene (12). Th22 and Th17 cells display reciprocal expression of the transcription factor T-bet and ROR $\gamma$ t, and, in Th22 cells, AHR cooperates with T-bet to boost IL-22 production (67). Thus, our results imply that AHR induces elaboration of T cell subtypes, in part through its direct role in inducing IL-23 production in myeloid cells, in addition to its downstream actions with ROR $\gamma$ t or T-bet to directly induce *IL22* gene expression.

In conclusion, our studies reveal that *M. tuberculosis* infection of macrophages induces AHR signaling, which has widespread effects on early innate immune responses to infection. AHR is highly expressed in barrier organs, such as the lung, and is activated by a number of ligands that are components of a healthy diet. Many current strategies for tackling TB aim to control active

**FIGURE 9.** Schematic representation of infection-induced Trp metabolism and AHR activation in macrophages and downstream events in T cells implicating signaling by macrophage-secreted IL-23 and IL-1 $\beta$ , as well as transactivation by AHR. See Discussion for details. *M.tb.*, *M. tuberculosis*.



disease or prevent progression of latent infection to disease. Another attractive point of intervention would be at the transition from exposure to infection by enhancing innate control at the time of exposure. Our results suggest that targeting AHR by dietary or other means in populations at high risk for exposure to *M. tuberculosis* might be an effective means to reduce rates of infection.

## Disclosures

The authors have no financial conflicts of interest.

## References

- Hooper, L. V. 2011. You AhR what you eat: linking diet and immunity. *Cell* 147: 489–491.
- Kiss, E. A., C. V. Conarbour, S. Kopfmann, E. Hobeika, D. Finke, C. Esser, and A. Diefenbach. 2011. Natural aryl hydrocarbon receptor ligands control organogenesis of intestinal lymphoid follicles. *Science* 334: 1561–1565.
- Esser, C., A. Rannug, and B. Stockinger. 2009. The aryl hydrocarbon receptor in immunity. *Trends Immunol.* 30: 447–454.
- Quintana, F. J. 2013. The aryl hydrocarbon receptor: a molecular pathway for the environmental control of the immune response. *Immunology* 138: 183–189.
- Munn, D. H., and A. L. Mellor. 2013. Indoleamine 2,3 dioxygenase and metabolic control of immune responses. *Trends Immunol.* 34: 137–143.
- Miniero, R., E. De Felip, F. Ferri, and A. di Domenico. 2001. An overview of TCDD half-life in mammals and its correlation to body weight. *Chemosphere* 43: 839–844.
- Kerkvliet, N. I. 2002. Recent advances in understanding the mechanisms of TCDD immunotoxicity. *Int. Immunopharmacol.* 2: 277–291.
- Henry, E. C., J. C. Bemis, O. Henry, A. S. Kende, and T. A. Gasiewicz. 2006. A potential endogenous ligand for the aryl hydrocarbon receptor has potent agonist activity in vitro and in vivo. *Arch. Biochem. Biophys.* 450: 67–77.
- Romani, L., F. Fallarino, A. De Luca, C. Montagnoli, C. D'Angelo, T. Zelante, C. Vacca, F. Bistoni, M. C. Fioretti, U. Grohmann, et al. 2008. Defective tryptophan catabolism underlies inflammation in mouse chronic granulomatous disease. *Nature* 451: 211–215.
- Taylor, M. W., and G. S. Feng. 1991. Relationship between interferon- $\gamma$ , indoleamine 2,3-dioxygenase, and tryptophan catabolism. *FASEB J.* 5: 2516–2522.
- Hughes, T. B., B. Becknell, A. G. Freud, S. McClory, E. Briercheck, J. Yu, C. Mao, C. Giovenzana, G. Nuovo, L. Wei, et al. 2010. Interleukin-1 $\beta$  selectively expands and sustains interleukin-22+ immature human natural killer cells in secondary lymphoid tissue. *Immunity* 32: 803–814.
- Qiu, J., J. J. Heller, X. Guo, Z. M. Chen, K. Fish, Y.-X. Fu, and L. Zhou. 2012. The aryl hydrocarbon receptor regulates gut immunity through modulation of innate lymphoid cells. *Immunity* 36: 92–104.
- Li, Y., S. Innocentin, D. R. Withers, N. A. Roberts, A. R. Gallagher, E. F. Grigorieva, C. Wilhelm, and M. Veldhoen. 2011. Exogenous stimuli maintain intraepithelial lymphocytes via aryl hydrocarbon receptor activation. *Cell* 147: 629–640.
- Mizoguchi, A. 2012. Healing of intestinal inflammation by IL-22. *Inflamm. Bowel Dis.* 18: 1777–1784.
- Shi, L. Z., N. G. Faith, Y. Nakayama, M. Suresh, H. Steinberg, and C. J. Czuprynski. 2007. The aryl hydrocarbon receptor is required for optimal resistance to *Listeria monocytogenes* infection in mice. *J. Immunol.* 179: 6952–6962.
- Monteleone, I., A. Rizzo, M. Sarra, G. Sica, P. Sileri, L. Biancone, T. T. MacDonald, F. Pallone, and G. Monteleone. 2011. Aryl hydrocarbon receptor-induced signals up-regulate IL-22 production and inhibit inflammation in the gastrointestinal tract. *Gastroenterology* 141: 237–248, e1.
- Moura-Alves, P., K. Faé, E. Houthuys, A. Dorhoi, A. Kreuchwig, J. Furkert, N. Barison, A. Diehl, A. Munder, P. Constant, et al. 2014. AhR sensing of bacterial pigments regulates antibacterial defence. *Nature* 512: 387–392.
- Dye, C. 2006. Global epidemiology of tuberculosis. *Lancet* 367: 938–940.
- Galagan, J. E. 2014. Genomic insights into tuberculosis. *Nat. Rev. Genet.* 15: 307–320.
- Keeler, E., M. D. Perkins, P. Small, C. Hanson, S. Reed, J. Cunningham, J. E. Aledort, L. Hillborne, M. E. Rafael, F. Girosi, and C. Dye. 2006. Reducing the global burden of tuberculosis: the contribution of improved diagnostics. *Nature* 444(Suppl. 1): 49–57.
- Marks, S. M., Z. Taylor, N. L. Qualls, R. J. Shrestha-Kuwahara, M. A. Wilce, and C. H. Nguyen. 2000. Outcomes of contact investigations of infectious tuberculosis patients. *Am. J. Respir. Crit. Care Med.* 162: 2033–2038.
- Khader, S. A., L. Gugliani, J. Rangel-Moreno, R. Gopal, B. A. Junecko, J. J. Fountain, C. Martino, J. E. Pearl, M. Tighe, Y. Y. Lin, et al. 2011. IL-23 is required for long-term control of *Mycobacterium tuberculosis* and B cell follicle formation in the infected lung. *J. Immunol.* 187: 5402–5407.
- Khader, S. A., S. Partida-Sanchez, G. Bell, D. M. Jelley-Gibbs, S. Swain, J. E. Pearl, N. Ghilardi, F. J. Desautels, F. E. Lund, and A. M. Cooper. 2006. Interleukin 12p40 is required for dendritic cell migration and T cell priming after *Mycobacterium tuberculosis* infection. *J. Exp. Med.* 203: 1805–1815.
- Khader, S. A., G. K. Bell, J. E. Pearl, J. J. Fountain, J. Rangel-Moreno, G. E. Cilley, F. Shen, S. M. Eaton, S. L. Gaffen, S. L. Swain, et al. 2007. IL-23 and IL-17 in the establishment of protective pulmonary CD4+ T cell responses after vaccination and during *Mycobacterium tuberculosis* challenge. *Nat. Immunol.* 8: 369–377.
- Verway, M., M. Bouttier, T.-T. Wang, M. Carrier, M. Calderon, B.-S. An, E. Devemy, F. McIntosh, M. Divangahi, M. A. Behr, and J. H. White. 2013. Vitamin D induces interleukin-1 $\beta$  expression: paracrine macrophage epithelial signaling controls *M. tuberculosis* infection. *PLoS Pathog.* 9: e1003407.
- Cingolani, P., A. Platts, L. Wang, M. Coon, T. Nguyen, L. Wang, S. J. Land, X. Lu, and D. M. Ruden. 2012. A program for annotating and predicting the effects of single nucleotide polymorphisms, SnpEff: SNPs in the genome of *Drosophila melanogaster* strain w1118; iso-2; iso-3. *Fly (Austin)* 6: 80–92.
- Zhang, Y., T. Liu, C. A. Meyer, J. Eeckhoutte, D. S. Johnson, B. E. Bernstein, C. Nusbaum, R. M. Myers, M. Brown, W. Li, and X. S. Liu. 2008. Model-based analysis of ChIP-Seq (MACS). *Genome Biol.* 9: R137.
- Ramirez-Gonzalez, R. H., R. Bonnal, M. Caccamo, and D. Maclean. 2012. Biosamtools: Ruby bindings for SAMtools, a library for accessing BAM files containing high-throughput sequence alignments. *Source Code Biol. Med.* 7: 6.
- Cingolani, P., V. M. Patel, M. Coon, T. Nguyen, S. J. Land, D. M. Ruden, and X. Lu. 2012. Using *Drosophila melanogaster* as a Model for Genotoxic Chemical Mutational Studies with a New Program, SnpSift. *Front. Genet.* 3: 35.
- Desvignes, L., and J. D. Ernst. 2009. Interferon-gamma-responsive non-hematopoietic cells regulate the immune response to *Mycobacterium tuberculosis*. *Immunity* 31: 974–985.
- Gandhi, R., D. Kumar, E. J. Burns, M. Nadeau, B. Dake, A. Laroni, D. Kozoriz, H. L. Weiner, and F. J. Quintana. 2010. Activation of the aryl hydrocarbon receptor induces human type 1 regulatory T cell-like and Foxp3(+) regulatory T cells. *Nat. Immunol.* 11: 846–853.
- Vogel, C. F., W. Li, D. Wu, J. K. Miller, C. Sweeney, G. Lazennec, Y. Fujisawa, and F. Matsumura. 2011. Interaction of aryl hydrocarbon receptor and NF- $\kappa$ B subunit RelB in breast cancer is associated with interleukin-8 overexpression. *Arch. Biochem. Biophys.* 512: 78–86.
- Lahoti, T. S., K. John, J. M. Hughes, A. Kusnadi, I. A. Murray, G. Krishnegowda, S. Amin, and G. H. Perdev. 2013. Aryl hydrocarbon receptor antagonism mitigates cytokine-mediated inflammatory signalling in primary human fibroblast-like synovocytes. *Ann. Rheum. Dis.* 72: 1708–1716.
- Martey, C. A., C. J. Baglione, T. A. Gasiewicz, P. J. Sime, and R. P. Phipps. 2005. The aryl hydrocarbon receptor is a regulator of cigarette smoke induction of the cyclooxygenase and prostaglandin pathways in human lung fibroblasts. *Am. J. Physiol. Lung Cell. Mol. Physiol.* 289: L391–L399.
- Vogel, C. F., S. R. Goth, B. Dong, I. N. Pessah, and F. Matsumura. 2008. Aryl hydrocarbon receptor signaling mediates expression of indoleamine 2,3-dioxygenase. *Biochem. Biophys. Res. Commun.* 375: 331–335.
- Thuong, N. T., S. J. Dunstan, T. T. Chau, V. Thorsson, C. P. Simmons, N. T. Quyen, G. E. Thwaites, N. Thi Ngoc Lan, M. Hibberd, Y. Y. Teo, et al. 2008. Identification of tuberculosis susceptibility genes with human macrophage gene expression profiles. *PLoS Pathog.* 4: e1000229.
- Doz, E., R. Lombard, F. Carreras, D. Buzoni-Gatel, and N. Winter. 2013. Mycobacteria-infected dendritic cells attract neutrophils that produce IL-10 and specifically shut down Th17 CD4 T cells through their IL-10 receptor. *J. Immunol.* 191: 3818–3826.
- Maerki, C., S. Meuter, M. Liebi, K. Mühlemann, M. J. Frederick, N. Yawalkar, B. Moser, and M. Wolf. 2009. Potent and broad-spectrum antimicrobial activity of CXCL14 suggests an immediate role in skin infections. *J. Immunol.* 182: 507–514.
- Schaerli, P., K. Willmann, L. M. Ebert, A. Walz, and B. Moser. 2005. Cutaneous CXCL14 targets blood precursors to epidermal niches for Langerhans cell differentiation. *Immunity* 23: 331–342.
- Yui, S., Y. Nakatani, and M. Mikami. 2003. Calprotectin (S100A8/S100A9), an inflammatory protein complex from neutrophils with a broad apoptosis-inducing activity. *Biol. Pharm. Bull.* 26: 753–760.
- Schröder, J. M., and J. Harder. 2006. Antimicrobial skin peptides and proteins. *Cell. Mol. Life Sci.* 63: 469–486.
- Peterson, L. W., and D. Artis. 2014. Intestinal epithelial cells: regulators of barrier function and immune homeostasis. *Nat. Rev. Immunol.* 14: 141–153.
- Buonocore, S., P. P. Ahern, H. H. Uhlig, I. I. Ivanov, D. R. Littman, K. J. Maloy, and F. Powrie. 2010. Innate lymphoid cells drive interleukin-23-dependent innate intestinal pathology. *Nature* 464: 1371–1375.
- Dhiman, R., M. Indramohan, P. F. Barnes, R. C. Nayak, P. Paidipally, L. V. Rao, and R. Vankayalapati. 2009. IL-22 produced by human NK cells inhibits growth of *Mycobacterium tuberculosis* by enhancing phagolysosomal fusion. *J. Immunol.* 183: 6639–6645.
- Peral de Castro, C., S. A. Jones, C. Ní Cheallaigh, C. A. Hearnden, L. Williams, J. Winter, E. C. Lavelle, K. H. Mills, and J. Harris. 2012. Autophagy regulates IL-23 secretion and innate T cell responses through effects on IL-1 secretion. *J. Immunol.* 189: 4144–4153.
- Creyghton, M. P., A. W. Cheng, G. G. Welstead, T. Kooistra, B. W. Carey, E. J. Steine, J. Hanna, M. A. Lodato, G. M. Frampton, P. A. Sharp, et al. 2010. Histone H3K27ac separates active from poised enhancers and predicts developmental state. *Proc. Natl. Acad. Sci. USA* 107: 21931–21936.
- Heintzman, N. D., R. K. Stuart, G. Hon, Y. Fu, C. W. Ching, R. D. Hawkins, L. O. Barrera, S. Van Calcar, C. Qu, K. A. Ching, et al. 2007. Distinct and predictive chromatin signatures of transcriptional promoters and enhancers in the human genome. *Nat. Genet.* 39: 311–318.
- Robertson, A. G., M. Bilenky, A. Tam, Y. Zhao, T. Zeng, N. Thiessen, T. Cezard, A. P. Fejes, E. D. Wederell, R. Cullum, et al. 2008. Genome-wide relationship between histone H3 lysine 4 mono- and tri-methylation and transcription factor binding. *Genome Res.* 18: 1906–1917.
- Shlyueva, D., G. Stampfel, and A. Stark. 2014. Transcriptional enhancers: from properties to genome-wide predictions. *Nat. Rev. Genet.* 15: 272–286.

50. Lan, X., H. Witt, K. Katsumura, Z. Ye, Q. Wang, E. H. Bresnick, P. J. Farnham, and V. X. Jin. 2012. Integration of Hi-C and ChIP-seq data reveals distinct types of chromatin linkages. *Nucleic Acids Res.* 40: 7690–7704.
51. Lusska, A., E. Shen, and J. P. Whitlock, Jr. 1993. Protein-DNA interactions at a dioxin-responsive enhancer. Analysis of six bona fide DNA-binding sites for the liganded Ah receptor. *J. Biol. Chem.* 268: 6575–6580.
52. Zhang, Y. J., M. C. Reddy, T. R. Ioerger, A. C. Rothchild, V. Dartois, B. M. Schuster, A. Trauner, D. Wallis, S. Galaviz, C. Huttenhower, et al. 2013. Tryptophan biosynthesis protects mycobacteria from CD4 T-cell-mediated killing. *Cell* 155: 1296–1308.
53. Russell, D. G. 2013. Trp'ing tuberculosis. *Cell* 155: 1209–1210.
54. Lowe, M. M., J. E. Mold, B. Kanwar, Y. Huang, A. Louie, M. P. Pollastri, C. Wang, G. Patel, D. G. Franks, J. Schlezinger, et al. 2014. Identification of cinnabarinic acid as a novel endogenous aryl hydrocarbon receptor ligand that drives IL-22 production. *PLoS One* 9: e87877.
55. Mayer-Barber, K. D., D. L. Barber, K. Shenderov, S. D. White, M. S. Wilson, A. Cheever, D. Kugler, S. Hieny, P. Caspar, G. Núñez, et al. 2010. Caspase-1 independent IL-1 $\beta$  production is critical for host resistance to mycobacterium tuberculosis and does not require TLR signaling in vivo. *J. Immunol.* 184: 3326–3330.
56. Fremont, C. M., D. Togbe, E. Doz, S. Rose, V. Vasseur, I. Maillet, M. Jacobs, B. Ryffel, and V. F. J. Quesniaux. 2007. IL-1 receptor-mediated signal is an essential component of MyD88-dependent innate response to *Mycobacterium tuberculosis* infection. *J. Immunol.* 179: 1178–1189.
57. Zhang, Y., M. Broser, H. Cohen, M. Bodkin, K. Law, J. Reibman, and W. N. Rom. 1995. Enhanced interleukin-8 release and gene expression in macrophages after exposure to *Mycobacterium tuberculosis* and its components. *J. Clin. Invest.* 95: 586–592.
58. Wilson, N. J., K. Boniface, J. R. Chan, B. S. McKenzie, W. M. Blumenschein, J. D. Mattson, B. Basham, K. Smith, T. Chen, F. Morel, et al. 2007. Development, cytokine profile and function of human interleukin 17-producing helper T cells. *Nat. Immunol.* 8: 950–957.
59. Khader, S. A., and A. M. Cooper. 2008. IL-23 and IL-17 in tuberculosis. *Cytokine* 41: 79–83.
60. Verreck, F. A., T. de Boer, D. M. Langenberg, M. A. Hoeve, M. Kramer, E. Vaisberg, R. Kastelein, A. Kolk, R. de Waal-Malefyt, and T. H. Ottenhoff. 2004. Human IL-23-producing type 1 macrophages promote but IL-10-producing type 2 macrophages subvert immunity to (myco)bacteria. *Proc. Natl. Acad. Sci. USA* 101: 4560–4565.
61. van de Vosse, E., M. A. Hoeve, and T. H. Ottenhoff. 2004. Human genetics of intracellular infectious diseases: molecular and cellular immunity against mycobacteria and salmonellae. *Lancet Infect. Dis.* 4: 739–749.
62. Cooper, A. M., A. Kipnis, J. Turner, J. Magram, J. Ferrante, and I. M. Orme. 2002. Mice lacking bioactive IL-12 can generate protective, antigen-specific cellular responses to mycobacterial infection only if the IL-12 p40 subunit is present. *J. Immunol.* 168: 1322–1327.
63. Juffermans, N. P., S. Florquin, L. Camoglio, A. Verbon, A. H. Kolk, P. Speelman, S. J. van Deventer, and T. van Der Poll. 2000. Interleukin-1 signaling is essential for host defense during murine pulmonary tuberculosis. *J. Infect. Dis.* 182: 902–908.
64. Yamada, H., S. Mizumo, R. Horai, Y. Iwakura, and I. Sugawara. 2000. Protective role of interleukin-1 in mycobacterial infection in IL-1 alpha/beta double-knockout mice. *Lab. Invest.* 80: 759–767.
65. Sonnenberg, G. F., L. A. Monticelli, T. Alenghat, T. C. Fung, N. A. Hutnick, J. Kunisawa, N. Shibata, S. Grunberg, R. Sinha, A. M. Zahm, et al. 2012. Innate lymphoid cells promote anatomical containment of lymphoid-resident commensal bacteria. *Science* 336: 1321–1325.
66. Guo, X., Y. Liang, Y. Zhang, A. Lasorella, B. L. Kee, and Y. X. Fu. 2015. Innate Lymphoid Cells Control Early Colonization Resistance against Intestinal Pathogens through ID2-Dependent Regulation of the Microbiota. *Immunity* 42: 731–743.
67. Basu, R., D. B. O'Quinn, D. J. Silberger, T. R. Schoeb, L. Fouser, W. Ouyang, R. D. Hatton, and C. T. Weaver. 2012. Th22 cells are an important source of IL-22 for host protection against enteropathogenic bacteria. *Immunity* 37: 1061–1075.
68. Ekins, S., Y. Nikolsky, A. Bugrim, E. Kirillov, and T. Nikolskaya. 2007. Pathway mapping tools for analysis of high content data. *Methods Mol. Biol.* 356: 319–350.